RESEARCH ARTICLE

Utility of scoring function customization in docking-based virtual screening approaches

Govardhan A. Balaji[1], Vitukudi N. Balaji[2] and Shashidhar N. Rao[3,4,*]

[1]Department of Chemistry, St Joseph's College, 36 Langford Road, Bangalore 560 027, India
[2]Structure Directed Molecular Design, Jubilant Biosys Ltd, #96, Industrial Suburb II Stage, Yeshwantpur, Bangalore 560 022, India
[3]Tripos – A Certara$_{TM}$ Company, 1699 South Hanley Road, St Louis MO 63144, USA
[4]Present address: Department of Chemistry and Chemical Biology, Rutgers University, Piscataway, NJ 08554, USA

Virtual screening of large chemical libraries plays a key role in lead identification and optimization in rational approaches to pharmaceutical drug discovery. Both ligand-based (e.g. 3D-QSAR) and structure-based (e.g. automated docking) methods are extensively used in such screening experiments. While the former techniques lead to good local models that rationalize the structure activity relations (SAR) in a given series, they provide limited insights into receptor–ligand interactions. Structure-based methods depend on scoring functions that are typically not functionalized to reproduce local SAR while doing a good job of producing accurate poses and enriching actives seeded in a decoy set. In this study, we have attempted to employ the ability to customize the scoring function associated with Surflex-dock technology to develop HIV-1 protease inhibitor-specific scoring functions using a well-defined training set of cyclic urea compounds. The study highlights the significance of various docking features such as protein flexibility, fragment-based core constraints and sampling of the docking space in optimization of docking scores. Applying customized scoring functions improved correlation between experimental and computed docking scores and thus enabled better rationalization of SAR. In addition, the tuned scoring functions show utility in recovery of actives in enrichment studies. Such studies lend themselves to identification of novel ligands as potential HIV-1 inhibitors from the pool of chemical libraries whose activities against HIV-1 protease are unknown.

Keywords: Cyclic urea inhibitors, docking protocol, HIV protease inhibitor, rational drug design.

VIRTUAL screening of large compound libraries is recognized to be an important component of modern pharmaceutical drug discovery[1–7]. It serves as a potential method for reducing downstream investment in valuable human and material resources needed for drug discovery and development, by eliminating untenable ligands early in the discovery process by rational criteria. Both ligand-based[3,8–10] and structure-based[1,8,10–12] three-dimensional virtual screening methods are popular and have been extensively developed and employed. The traditional ligand-based approaches such as 3D-QSAR are useful in the development of focused local models that rationalize experimental observations in and around a given chemical series[2,3,13]. However, they are dependent on the quality of molecular alignments stemming from the assumption of a common binding mode between the members of a dataset of molecules[14–16]. Such alignments in turn are dependent on the nature and sampling of the conformational spaces of the molecules. Despite their utility in rationalizing local structure–activity effects, the ligand-based 3D-QSAR models are limited in their scope as they do not offer any significant insights into interactions with receptor structure active site/s. By contrast, the traditional structure-based methods such as docking offer considerable insights into receptor–ligand interactions and help rationalize the structure–activity relations (SAR) in terms of the emphasis on such interactions. However, the biggest challenge in the field of docking and scoring is the utilization of scoring functions which rank order different energetically feasible poses obtained by using conventional energy force field approaches[17–23]. Specifically, various scoring functions are tuned for docked pose accuracy and enrichment of actives, but not necessarily geared toward reproducing ranking of experimentally observed binding data[24–31]. Any correlations are generally deemed accidental rather than being obtained by design. This limitation presents considerable challenges in the area of structure-based lead optimization of chemical series.

In recent years, several molecular dynamics, Watermap, free energy perturbation (FEP), molecular mechanics – generalized born model augmented with solvent accessible surface area (MMGB/SA) and molecular mechanics – Poisson Boltzmann surface area (MMPB/SA) methods have been studied to develop computational approaches to improve binding affinity predictions[32–37]. However, the success of such methods is dependent upon considerable degree of parameterization and tweaking of protocols and is consequently not practical in the context of high-throughput drug discovery processes due to (a) limitations in the force field representations of various complex interactions involving receptor, ligand/s and solvent molecules, (b) limitations in the sampling of the conformational spaces of receptor–ligand–solvent complexes, (c) long simulation times and (d) lack of transfer-

*For correspondence. (e-mail: shashidharr@gmail.com)

ability of protocols to systems significantly different from the ones for which initial optimizations are done.

In this study, we have investigated the utility of scoring function customization feasible through the Surflex-dock[24,29] approach to examine if such customization can improve upon the correlation between experimental binding affinities and docking scores. To the best of our knowledge, Surflex-dock is the only docking technology which allows out-of-the-box ability to customize scoring function toward reproducing experimental binding affinities. As an example, we have used a focused training set of nine isomers of a cyclic urea-based HIV-1 protease inhibitor[38] to carry out such a customization using a variety of computational protocols involving protein side chain and main chain flexibility, sampling level of docking space and fragment-based core constraints. The HIV-1 protease inhibitory activities of these compounds span more than three orders of magnitude. We have demonstrated that the customized scoring functions do lead to improvements in correlations between experimentally observed binding affinities and docking scores. We have used some of the customized scoring functions to carry out enrichment studies to analyse their impact on retrieving a set of active cyclic urea-based HIV-1 protease inhibitors seeded in a HIV-specific decoy dataset obtained from DUD (**http://dud.docking.org**). We find that the customized scoring functions do lead to marginal improvements in the enrichment of active ligands. Thus, it appears that chemotype-specific scoring function customization may be a useful alternative strategy to more expensive simulations-based approaches involving molecular dynamics and FEP methods.

Materials and methods

Target protein, data sets and molecular modelling

All the docking studies were carried out using the protein–ligand complex with crystal structure entry with code 1QBT[39] (Protein Data Bank – http://www.pdb.org)[40]. The ligand containing a seven-membered ring cyclic urea, in this complex is a potent inhibitor of HIV-1 protease (binding K_i of 0.024 nM)[39]. There are no X-ray crystallographic water molecules in this complex as the urea moiety displaces the active-site water present in the bound complex of HIV-1 with peptidic inhibitors (e.g. the PDB code 4PHV)[40,41]. This complex was employed as input for protein preparation in Sybyl-X (version 1.3)[37]. Hydrogen atoms were added to the protein–ligand complex and the terminal residues were maintained in their charged states (NH_3^+ and COO^-). All the amide moieties in the side chains of asparagine and glutamine were adjusted to optimize their interactions with surrounding residues and groups of atoms. The protonation states of the two histidines were retained at their default values of HID (hydrogen on the N^δ atom) since they are beyond the 8 Å shell around the ligand. The protein–ligand complex was subjected to 'staged minimization' which consisted of the following steps: (i) minimization of hydrogen positions, (ii) minimization of side chain atoms, (iii) minimization of the entire protein structure minus the C^α atoms, (iv) minimization of the ligand and (v) minimization of all the atoms. In each step, 100 cycles of steepest descent and conjugate gradient energy minimizations were carried out using the Tripos force field[42]. It should be noted that the main goal of this 'staged minimization' is to clean up the original X-ray structure after the addition of hydrogen atoms and reorientation of the asparagine and glutamine side-chain amides. Thus, the above procedure maintains the integrity of the experimental structure of 1QBT as noted by the value of 0.2 Å for the root mean square deviation (RMSD) of the heavy atoms between the minimized and X-ray protein atoms. As noted above, this PDB entry did not contain any crystallographic water molecules in the protein–ligand complex and is suitable for docking cyclic urea inhibitors, which have been studied here.

The cyclic urea ligands (Figure 1) used in the principal docking studies, referred to henceforth as TRGSET, were taken from Kaltenbach *et al.*[38] and prepared using the 'Ligand Preparation' panel in Sybyl-X[37]. The molecules were input in the form of 2D structures (drawn in ChemDraw), stored in SDF formatted file and subject to co-ordinate generation by CONCORD[43], within the Ligand Preparation module. It should be mentioned that CONCORD generated structures have stereochemically acceptable bond lengths and bond angles which do not vary during the docking simulations. These structures are however endowed with reasonable dihedral angles which do vary during the flexible docking of ligands.

In addition to the set of these nine ligands, we also prepared a collection of active HIV-1 protease inhibitors containing six- and seven-membered cyclic ureas[39,44–58] (Table 1) referred to henceforth as TESTSET1, an external test set of 71 HIV-1 protease inhibitors spanning

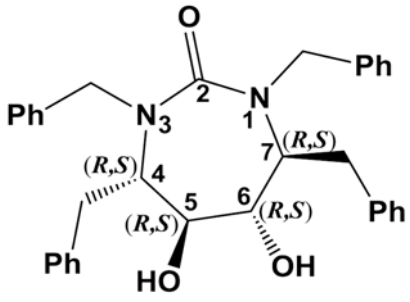

Figure 1. Schematic illustration of TRGSET members (compounds **1** through **9**) investigated in the docking studies. The stereochemistry at atoms **4**–**7** in these compounds is as follows: **1** (RSSR), **2** (RSRR), **3** (RSSS), **4** (RSRS), **5** (SSSS), **6** (RRRR), **7** (SRSS), **8** (SRRS) and **9** (SRRR). Experimentally measured binding affinities (in terms of K_i values) for these compounds are as follows: **1** (3.6 nM), **2** (6.0 nM), **3** (64 nM), **4** (250 nM), **5** (560 nM), **6** (1350 nM), **7** (1710 nM), **8** (3810 nM) and **9** (6700 nM).

Table 1. Active inhibitors of HIV-1 protease* used in the enrichment studies

Ligand	K_i	pK_i	Reference	Ligand	Ki	pK_i	Reference
CHEMBL85653	0.010	11.000	45	CHEMBL312796	0.016	10.796	48
CHEMBL309629	0.010	11.000	48	CHEMBL311474	0.016	10.796	48
CHEMBL73240	0.010	11.000	52, 55	CHEMBL412862	0.016	10.796	36
CHEMBL316681	0.010	11.000	52	CHEMBL434098	0.018	10.745	52
CHEMBL405187	0.010	11.000	45, 54	CHEMBL431174	0.018	10.745	49
CHEMBL81383	0.010	11.000	45, 54	CHEMBL79149	0.018	10.745	48
CHEMBL305125	0.010	11.000	49	CHEMBL316147	0.018	10.745	45, 54
CHEMBL36900	0.010	11.000	53	CHEMBL420944	0.018	10.745	48
CHEMBL70626	0.011	10.959	55	CHEMBL78671	0.018	10.745	48, 52
CHEMBL133292	0.012	10.921	47	CHEMBL320005	0.018	10.745	44
CHEMBL313348	0.012	10.921	54	CHEMBL262642	0.018	10.745	45, 54, 47
CHEMBL313959	0.014	10.854	45, 54	CHEMBL284942	0.018	10.745	48, 46
CHEMBL291677	0.014	10.854	45, 54, 48, 36	CHEMBL262378	0.020	10.699	45, 54
CHEMBL408834	0.016	10.796	45, 54	CHEMBL315929	0.020	10.699	45, 54
CHEMBL427992	0.016	10.796	51	CHEMBL116517	0.020	10.699	53
CHEMBL133291	0.016	10.796	47	CHEMBL416783	0.020	10.699	53
CHEMBL315569	0.016	10.796	54	CHEMBL413332	0.021	10.678	57
CHEMBL349637	0.016	10.796	50	CHEMBL312366	0.021	10.678	48
CHEMBL61173	0.021	10.678	49	CHEMBL366576	0.060	10.222	53
CHEMBL312349	0.022	10.658	48	CHEMBL78504	0.027	10.569	48
CHEMBL336730	0.023	10.638	47	CHEMBL85990	0.027	10.569	45, 54
CHEMBL313288	0.023	10.638	54	CHEMBL57375	0.027	10.569	45, 54, 36, 48
CHEMBL288254	0.023	10.638	48, 53	CHEMBL38314	0.027	10.569	53, 49, 50
CHEMBL89064	0.024	10.620	54	CHEMBL312659	0.028	10.553	48
CHEMBL131268	0.024	10.620	47	CHEMBL310125	0.029	10.538	48
CHEMBL11266	0.024	10.620	45, 54, 36, 48, 51	CHEMBL82422	0.030	10.523	48, 56
CHEMBL57707	0.025	10.602	36	CHEMBL286671	0.030	10.523	53
CHEMBL86398	0.025	10.602	45, 54	CHEMBL291004	0.030	10.523	53
CHEMBL80182	0.025	10.602	48	CHEMBL290331	0.060	10.222	53
CHEMBL408252	0.026	10.585	51	CHEMBL416612	0.060	10.222	53

*The three-dimensional coordinates of these inhibitors are available in a SD formatted file provided by the authors as '**Supplementary material**'.

more than four orders of magnitude, referred to henceforth as TESTSET2 (Table 2) and a set of HIV-1 specific decoy ligands obtained from DUD database. The criterion for choosing TESTSET1 compounds was a pK_i (computed as $9 - \log_{10}[K_i]$) cut-off of 10 ($K_i < 100$ picomolar) in the HIV-1 protease binding assay. The TESTSET2 compounds were chosen from a collection of 426 cyclic urea inhibitors of HIV-1 protease reported in the literature by the application of the SELECTOR module of Sybyl-X[37]. This method was employed to select a sixth of the dataset representing diversity in the chemical and biological spaces of the ligands. In the preparation of these three sets of ligands, stereochemistry was expanded wherever it was not originally specified and all possible ionization and tautomer states were generated using environment-specific rules, as applicable.

The prepared HIV-1 protease–ligand 1QBT complex (vide supra) was used as input in Surflex-dock module of Sybyl-X to generate a 'protomol' using the 'Ligand' option. It may be noted that the centroid of the ligand coordinates is used as a starting point for identification of potential sites in the active site which can be occupied by ligand functional groups. The protomol consists of a collection of clustered probes that represent hydrophobic (methane) and hydrophilic (NH and C=O) interactions with the protein atoms[26]. Thus, the protomol represents the fingerprint of an active site and was employed in docking the prepared ligands (vide supra).

The prepared TRGSET compounds were docked into 1QBT using all the four docking modes (Default, Screen, GEOM and GEOMX) available through the Surflex-dock[24,28,32,36,59], interface in Sybyl-X. For each of these docking modes, docking calculations were carried out in two sets of conditions – (i) with and without the incorporation of protein flexibility and (ii) with and without the incorporation of placed fragment constraints. In docking experiments where protein flexibility is incorporated, all hydrogen atoms and heavy atoms within 8 Å of ligand poses are allowed to undergo movements. In docking runs with placed fragment constraints, the three-dimensional coordinates of the seven-membered urea core (Figure 1) were specified as positional constraints with a penalty value of 40 kcal/mol/Å. For the sake of reference, the atoms in the seven-membered rings will be referred to by their numbers as shown in Figure 1. The docked poses were required to 'match the fragment' implying that the 3D coordinates of the fragment in the former were similar to the corresponding coordinates in the X-ray structure of 1QBT. Ligand ring flexibility was explored in all GEOMX docking calculations in which

Table 2. Experimental pK_i and docking scores obtained by 'Default mode' Surflex docking using the default (column 3) and customized scoring functions (columns 4 to 6) for the HIV-1 protease inhibitors in TESTSET2

Ligand	Expt. pK_i	Default	GEOM_CC_NPF	GEOMX_CC_NPF	GEOMX_NCC_NPF	Reference
CHEMBL68086	6.310	8.402	7.085	6.558	7.107	60
CHEMBL97836	6.839	8.031	7.451	7.074	7.226	58
CHEMBL98826	7.046	8.150	6.004	7.218	7.855	58
CHEMBL89064	7.066	8.864	7.626	7.744	7.884	54
CHEMBL431027	7.284	8.082	6.507	8.235	6.946	45, 54
CHEMBL431174	7.292	10.880	8.491	8.368	7.480	49
CHEMBL335651	7.377	9.060	7.929	6.439	6.613	45
CHEMBL99013	7.456	11.261	7.718	7.128	6.344	58
CHEMBL339147	7.495	10.338	8.892	7.812	8.541	47
CHEMBL166604	7.523	8.670	7.572	6.199	6.459	50
CHEMBL291677	7.538	11.047	8.034	8.886	8.701	45,54, 48, 39
CHEMBL413332	7.658	9.885	8.460	8.078	7.993	57
CHEMBL421730	7.854	9.535	7.379	6.861	7.970	45, 54
CHEMBL409292	7.886	9.720	7.304	7.191	7.392	61
CHEMBL353484	7.914	11.322	8.546	7.550	8.633	50
CHEMBL167005	7.921	7.834	6.558	6.548	6.459	50
CHEMBL420944	8.051	11.706	8.424	8.526	8.436	48
CHEMBL99174	8.076	10.298	8.094	8.444	8.756	58
CHEMBL315300	8.149	7.527	7.131	7.893	7.860	54, 62
CHEMBL166936	8.155	10.331	9.353	7.981	8.839	50
CHEMBL312562	8.155	11.134	9.474	8.837	9.166	48
CHEMBL303151	8.194	9.894	8.318	7.428	8.768	60
CHEMBL431552	8.215	10.616	8.844	8.205	9.527	60
CHEMBL322991	8.244	12.076	9.561	8.516	9.532	56
CHEMBL428348	8.284	11.701	8.654	8.217	9.427	51
CHEMBL420042	8.284	10.563	9.259	8.398	9.231	54, 62
CHEMBL346818	8.319	9.038	8.062	7.773	7.899	57
CHEMBL60352	8.444	7.303	7.307	8.808	7.438	49
CHEMBL132175	8.444	8.694	7.955	8.183	8.955	47
CHEMBL89132	8.523	9.993	7.823	8.563	8.687	45, 54
CHEMBL74625	8.523	11.121	8.275	8.784	9.215	55
CHEMBL310124	8.602	10.913	9.376	8.039	8.624	48
CHEMBL137526	8.620	11.328	9.986	9.001	9.048	45
CHEMBL154962	8.658	11.528	9.153	9.250	9.355	57
CHEMBL415040	8.721	9.341	7.493	7.802	8.449	54, 62, 63
CHEMBL107648	8.745	11.912	9.491	8.657	9.695	56
CHEMBL280990	8.796	10.781	8.632	8.399	8.432	61
CHEMBL107817	8.796	11.327	10.004	9.831	8.761	56
CHEMBL109377	8.824	10.692	9.058	8.075	8.375	56
CHEMBL432566	8.886	9.521	7.726	8.390	8.028	54
CHEMBL34661	9.032	10.701	9.471	9.161	7.617	64
CHEMBL70626	9.051	8.889	8.169	7.925	8.559	55
CHEMBL302864	9.066	10.693	8.583	8.146	7.817	49
CHEMBL293654	9.066	11.745	9.429	8.198	9.274	49
CHEMBL79023	9.130	9.866	9.386	8.441	7.751	48
CHEMBL29342	9.155	9.486	7.834	7.753	7.738	61
CHEMBL302585	9.155	9.527	8.008	7.736	8.159	60
CHEMBL108932	9.194	11.367	9.810	8.786	9.326	56
CHEMBL415071	9.387	11.188	9.093	8.747	8.870	55
CHEMBL294582	9.398	8.942	8.239	8.415	8.117	49
CHEMBL81514	9.432	12.873	9.144	9.234	9.511	48
CHEMBL311474	9.509	10.718	8.064	8.153	8.244	48
CHEMBL82422	9.538	11.265	9.759	9.085	9.700	48, 56
CHEMBL34019	9.638	11.759	9.910	9.088	9.623	64
CHEMBL78949	9.678	11.007	9.515	8.936	10.196	48
CHEMBL29089	9.699	9.559	9.298	8.255	8.809	61
CHEMBL311267	9.699	10.052	9.922	10.543	9.811	48
CHEMBL431702	9.721	8.601	8.347	8.511	8.724	60, 64
CHEMBL433136	9.770	10.457	8.653	8.285	8.521	48
CHEMBL87835	9.770	11.981	10.005	9.034	9.225	45, 54

(*Contd*)

Table 2. (*Contd*)

Ligand	Expt. pK_i	Default	GEOM_CC_NPF	GEOMX_CC_NPF	GEOMX_NCC_NPF	Reference
CHEMBL73240	9.921	11.856	8.577	8.704	9.122	52, 55
CHEMBL308568	10.161	11.553	9.799	9.048	9.545	55
CHEMBL311079	10.174	9.930	10.060	9.255	9.387	48
CHEMBL312672	10.208	9.621	9.777	9.280	9.518	48
CHEMBL312349	10.319	11.955	9.944	9.578	9.930	48
CHEMBL312030	10.328	11.598	11.053	8.984	10.049	48
CHEMBL280989	10.337	10.973	9.394	9.272	9.281	61
CHEMBL28558	10.509	11.752	9.651	9.253	10.170	61
CHEMBL316407	10.523	12.392	9.964	9.842	10.022	54
CHEMBL410740	10.620	12.945	11.234	10.649	10.724	51
CHEMBL312796	10.699	14.433	11.781	11.475	11.880	48

The three-dimensional coordinates of these 71 inhibitors are available in a SD (structure-data) formatted file provided by the authors as '**Supplementary material**'.

'placed fragment' constraint was not employed. In each docking experiment, up to 20 poses were saved for each of the nine ligands in TRGSET based on their 'total docking score' values. The top-ranked docked poses for each of the ligands were analysed for intermolecular (protein–ligand) hydrogen bonds using the 'Results Browser' of the Surflex-dock GUI in Sybyl-X. Correlation plots with experimental pK_i values represented on the *X*-axis and total docking score on the *Y*-axis were generated within Microsoft Excel.

Results and discussion

Docking of TRGSET molecules

Using the 'Results Browser', the top five poses of each ligand were saved in Sybyl Line Notation formatted files which were used as input for scoring function customization, previously described in Pham and Jain[29], using the command line execution mode. The command line optimization of the scoring function was executed over five iterations using the option '+misc_remin' to turn on all-atom energy minimization. The scoring function optimization was tuned by the inclusion of 34 scoring constraints corresponding to the experimental binding affinities of ligands in training set complexes. This was done to prevent potential over-training of the scoring function in favour of TRGSET members. The docked pose constraints were weighted by a factor of five relative to the training set constraints. At the end of customization, docking scores corresponding to the customized parameters are reported for each input ligand pose. For the sake of further discussions, the customized scores will be referred to as custom docking score (CDS). Since five poses were used for each ligand, correlation factors were computed using the following five protocols to obtain an objective metric of validation: (i) CDS of the top-ranked pose; (ii) highest value of CDS; (iii) lowest value of the CDS; (iv) mean of the highest and the lowest CDS values and (v) average of all five CDS values.

High-throughput docking studies (using the default Surflex-dock and GEOM docking modes) were carried out to determine the enrichment of active ligands that are seeded in a database of decoy molecules. As stated earlier, the TESTSET1 ligands were seeded into a HIV-1 protease-specific DUD decoy database of 1885 compounds available as **supplementary material**. These docking studies were carried out using the default set of parameters and three customized sets of parameters derived from the scoring function customization experiment. Default settings were used in all these calculations aimed at realizing the enrichment of actives. Thus, no protein flexibility was incorporated and no placed fragment constraints were employed. Enrichment plots indicating the cumulative percentages of actives (*Y*-axis) in increasing percentages of database (*X*-axis) were drawn using Microsoft Excel.

All the top-ranked docked poses of the ligands in TRGSET have interactions with HIV-1 protease, which are generally consistent with the interaction patterns seen for the ligand in the X-ray complex 1QBT. Figure 2 illustrates the profile of interactions between the top-ranked pose of compound **1** (the most active of the TRGSET members) with the active-site residues of HIV-1 protease. These interactions include two (N–H···O) hydrogen-bond interactions between the carbonyl group of the cyclic urea (Figure 1) on the one hand and the backbone N–H moieties of active site residues Ile50 from chains A and B on the other. Furthermore, the side chain carboxylates of the catalytic residues Asp25 from chains A and B form strong O–H···O hydrogen-bonding interactions with the hydroxyl groups attached to two of the carbons (atoms 5 and 6 in Figure 1) in the cyclic urea moiety of compound **1**.

In addition to these hydrogen-bonding interactions, the top-ranked pose of compound **1** is stabilized in the active site by hydrophobic interactions experienced by the benzyl moieties substituted on the two nitrogen atoms of the cyclic urea as well as those substituted on carbon atoms numbered 4 and 7 in Figure 1. In fact, as illustrated in Figure 3, these moieties overlap nicely on top of the

corresponding benzyl moieties in the X-ray ligand of 1QBT and form hydrophobic interactions with the side chains of a number of valine and isoleucine residues lining the active site, including Ile50, Ile84, Val82, Ala29 and Pro81. It is gratifying to note that the average RMSDs of the benzyl moiety atoms relative to the corresponding atoms in the X-ray ligand are less than 1 Å. Figure 4 shows the overlap of the top-ranked poses of compounds **1** and **2**, which are the two most active compounds in the training set TRGSET, in the active site of the 1QBT protein. These poses were computed using the GEOMX docking mode without core constraints and protein flexibility. The overlap of these poses with the X-ray ligand is shown in Figure 3, which clearly illustrates the similarity in the location of the cyclic urea moiety of the top-ranked docked poses relative to that of the X-ray ligand (RMSD values of less than 0.8 Å). The remaining seven molecules in TRGSET (3 to 9) dock in the active site with generally larger variations in the locations of the urea and the benzyl moieties relative to the X-ray ligand. An example of such variations is shown in Figure 5 which illustrates the overlap of top-ranked docked poses obtained by GEOMX mode of docking without the application of core constraints and protein flexibility.

Notwithstanding these variations, all the top-ranked docked poses are involved in hydrogen-bonding interactions with the main chain NH of Ile50 and side chain carboxylates of Asp25 from both the chains as described above in the case of the top-ranked docked poses of compounds **1** and **2**. Further evidence of these interactions is seen in the bunching together of the urea carbonyl group and the pendant hydroxyls (Figure 5).

The conservation of the key interactions with the active site amino acid residues by various top-ranked docked

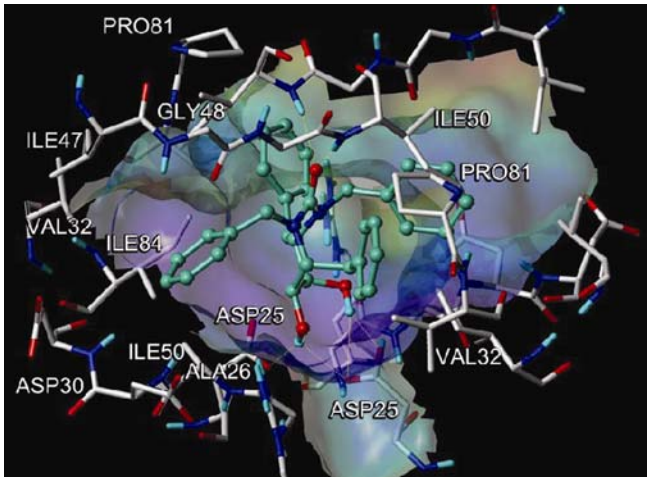

Figure 2. Computer graphic illustration of hydrogen-bonding interactions between the top-ranked docked pose of compound **1** in the active site of HIV-1 protease (from 1QBT). Hydrophobic packing interactions of the ligand phenyl rings against the side chain atoms of Ile84, Ile50 and Pro81 are also evident.

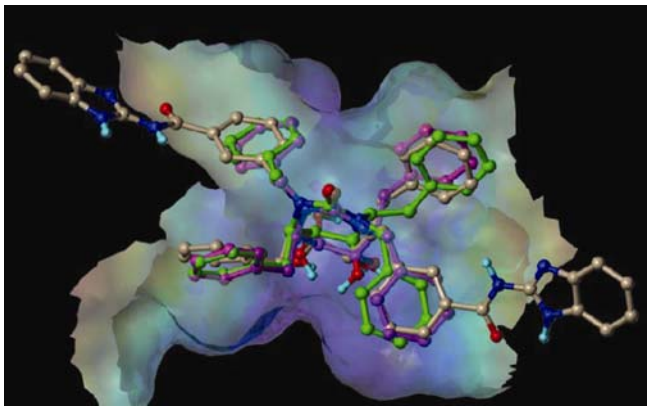

Figure 3. Overlap of the top-ranked docked poses of compounds **1** and **2** with the X-ray structure of 1QBT ligand in the active site of HIV-1 protease of 1QBT.

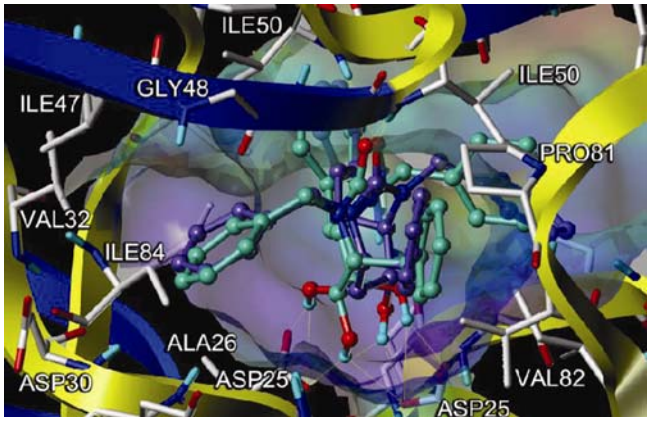

Figure 4. Overlap of the top-ranked poses of compounds **1** and **2**, in the active site of the 1QBT protein. Hydrogen-bonding interactions of the ligand hydroxyl groups with Asp25 side chain atoms (from both chains) are evident despite the change in stereochemistry for one of the hydroxyl groups.

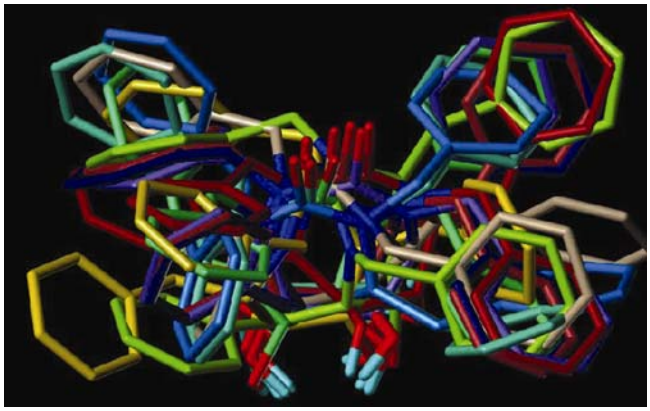

Figure 5. Overlap of the top-ranked docked poses of compounds **1** through **9** in the active site of HIV-1. All the carbonyl oxygen atoms in the cyclic urea interact with the backbone NH moieties of Ile50 from either chain, while the hydroxyl moieties at C-5 and C-6 interact with Asp25 side chain carboxylate of either chain. The hydrophobic regions of the ligands have interactions similar to those depicted in Figure 4.

Table 3. Root mean square deviations (RMSD; in Å) of the top-ranked docked poses relative to the common core atoms in the 1QBT ligand

		Stereochemistry (molecule number)*									
Docking mode	Constraints	RSSR (1)	RSRR (2)	RSSS (3)	RSRS (4)	SSSS (5)	RRRR (6)	SRSS (7)	SRRS (8)	SRRR (9)	Average RMSD
DEFAULT	CC + NPF	0.2	1.3	0.19	1.31	0.61	1.3	0.87	1.3	1.32	0.93
	CC + PF	0.28	0.29	0.38	0.19	1.28	0.31	1.31	0.34	1.02	0.60
	NCC + NPF	0.28	1.28	0.96	0.83	0.91	1.31	0.25	1.32	0.82	0.88
	NCC + PF	0.35	0.31	1.31	0.25	1.19	1.28	0.58	1.3	0.27	0.76
GEOM	CC + NPF	0.37	0.3	1.31	0.79	1.28	0.24	1.28	1.28	0.93	0.86
	CC + PF	0.44	0.29	0.53	0.41	1.3	1.31	1.21	1.29	0.96	0.86
	NCC + NPF	0.44	1.28	0.2	0.41	0.87	0.93	0.89	1.29	1.29	0.84
	NCC + PF	0.81	0.29	0.66	1.07	0.87	0.36	0.24	0.28	0.21	0.53
GEOMX	CC + NPF	1.29	0.3	0.23	1.37	0.87	1.26	0.89	1.23	0.34	0.86
	CC + PF	1.3	0.2	0.26	0.27	1.33	1.3	0.87	1.3	0.25	0.79
	NCC + NPF	1.3	0.2	1.32	0.27	0.28	1.3	0.82	1.3	0.26	0.78
	NCC + PF	1.3	1.28	0.26	1.35	0.97	1.31	0.25	0.16	0.25	0.79
SCREEN	CC + NPF	1.3	1.29	0.19	1.31	1.29	0.22	1.3	1.31	0.92	1.01
	CC + PF	1.3	1.29	0.62	0.58	0.3	0.22	0.79	1.29	0.92	0.81
	NCC + NPF	1.31	1.3	0.9	0.18	0.61	1.27	0.85	1.31	1.32	1.01
	NCC + PF	1.35	1.65	0.18	0.41	1.16	1.57	1.29	0.35	1.16	1.01

*See Figure 1.

Table 4. Correlation factors (last row) between the experimental pK_i values of compounds **1** through **9** (TRGSET) listed in column 2 and computed docking scores using various computational protocols listed in columns 3 to 18. Subscripts 1–4 correspond to the following combinations: 1, Core constraints and no protein flexibility; 2, Core constraints and protein flexibility; 3, No core constraints and no protein flexibility, and 4, No core constraints and protein flexibility. Docking scores corresponding to GEOM (G), GEOMX (GX), SCREEN (SCR) and DEFAULT (DEF) modes of docking are shown in columns 3–6, 7–10, 11–14 and 15–18 respectively

		Scoring function customization: docking modes and parameters															
		GEOM (G)				GEOMX (GX)				SCREEN (SCR)				DEFAULT (DEF)			
Compound*	pK_i	G_1	G_2	G_3	G_4	GX_1	GX_2	GX_3	GX_4	SCR_1	SCR_2	SCR_3	SCR_4	DEF_1	DEF_2	DEF_3	DEF_4
1	8.44	7.95	8.48	7.63	6.91	8.15	7.44	8.13	8.63	7.95	6.24	6.32	7.88	7.95	6.90	6.77	5.30
2	8.22	8.56	8.34	8.41	7.91	8.45	7.94	8.56	7.93	8.17	6.17	8.27	6.17	8.30	6.57	8.27	6.22
3	7.19	7.67	8.56	7.83	7.53	8.52	7.44	7.89	8.20	7.83	7.52	7.34	7.52	8.11	7.52	7.34	7.52
4	6.60	7.78	6.57	7.86	7.66	8.58	7.00	8.58	7.11	7.03	6.28	6.69	7.18	7.09	7.46	6.85	7.69
5	6.25	7.43	7.14	7.84	5.69	7.91	6.56	8.03	6.45	7.65	6.57	6.34	5.83	7.65	7.80	6.58	7.36
6	5.87	7.92	6.04	7.92	6.21	9.15	6.12	7.97	5.66	8.08	6.91	7.92	6.05	7.39	6.91	7.92	6.91
7	5.77	8.10	7.68	8.10	7.26	8.10	7.32	8.55	7.26	8.10	5.60	8.10	4.27	8.10	6.76	8.10	6.76
8	5.42	8.12	7.18	7.60	6.86	8.12	7.01	7.46	7.21	7.64	7.69	7.17	7.86	7.64	6.27	7.17	7.58
9	5.17	7.61	7.12	7.50	7.12	7.98	6.23	7.98	6.78	7.09	6.60	6.48	5.94	6.73	7.89	6.49	6.19
Correlation (R)→		0.37	0.69	0.39	0.37	0.13	0.74	0.38	0.74	0.42	–0.24	0.04	0.38	0.62	–0.18	0.17	–0.47

*See Figure 1.

poses is consistent with their RMSD values relative to the common core atoms found in the X-ray pose of the 1QBT ligand. All the 38 heavy atoms in ligands **1** through **9** are common to the 1QBT ligand and their 'in-place' RMSD values in the top-ranked docked poses are listed in Table 3 in each docking protocol described above. As seen from Table 3, all the RMSD values are less than 2 Å and the average RMSD values across the nine compounds are fairly insensitive to the docking protocol. For example, the RMSD values obtained for top-ranked poses with default docking mode are similar to those obtained by the more time-expensive GEOM and GEOMX docking modes. The lowest RMSD values are obtained with GEOM docked top-ranked poses in a protocol incorporating protein flexibility but no core constraints.

A key question that we have addressed in these studies is how well the Surflex-dock scores of the top-ranked docked poses of compounds **1** to **7** correlate with their measured pK_i values of HIV-1 protease inhibition. Toward this end, we have computed the Pearson-R (correlation) factors between the experimental pK_i and computed total score values in Surflex-dock (Table 4). As seen from Table 4, docking with GEOMX and incorporation of post-docking protein flexibility (PDPF) leads to

the highest correlation factor value of 0.74. This correlation seems to be independent of whether core constraints are included or excluded in the docking of the TRGSET compounds. By contrast, the correlation is much poorer when post-docking protein flexibility is not included, as seen by the correlation values of 0.14 and 0.38. Comparable correlation value ($R = 0.69$) is also observed with GEOM docked poses when protein flexibility is incorporated along with the application of core constraints. However, the correlation is much poorer with GEOM docking when post-docking protein flexibility is employed while not applying core constraints. Most of the docking experiments using the default mode and screening mode led to poor correlation between experimental pK_i values and docking scores of top-ranked poses. Surprisingly, in the default mode of docking a correlation factor of 0.62 is observed for poses generated with core constraints and no post-docking protein flexibility, whereas introducing this flexibility worsens the correlation to –0.18. Thus, it appears that docking scores generally do not correlate well with experimentally observed pK_i values despite the accuracy of the docking modes of the top-ranked poses, unless post-docking protein flexibility is included. This is not entirely surprising since the Surflex-dock scoring function in its default implementation is guided by two metrics – pose prediction accuracy and enrichment of actives seeded in a decoy dataset. Indeed, as discussed earlier the docking accuracy is reproduced for the TRGSET compounds. Also, HIV-1 protease active inhibitors seeded in the DUD decoy set of 1885 compounds are recovered with good enrichments, as illustrated in Figures 6 and 7, where the percentage of actives recovered (*Y*-axis) are plotted as a function of percentage of database screened (*X*-axis). In the plots, the red (Figure 6) and blue (Figure 7) coloured curves correspond to virtual screening using the default and GEOM docking modes respectively. As is evident in the plots, in the case of GEOM mode screening, more than 90% of the active compounds is recovered within the top 5% of the total database (enrichment factor of 18). All the actives are recovered within 22% of the total database leading to a minimum enrichment of 4.55. On the other hand, two-thirds of the active compounds are recovered in the top 5% of the total database in the screening by default docking mode (enrichment factor of 13.4), while 90% of the actives is recovered in 60% of the total dataset (enrichment factor of 1.5). Both methods recover about 32% of the active compounds in 1% of the total database. These results indicate that a substantial number of actives is recovered in a small fraction (e.g. 1% to 5%) with significant enrichment. Such enrichments, reflected by their area under the curve (AUC) values of 0.84 and 0.90 respectively, are useful sources of lead identification in pharmaceutical drug discovery workflows.

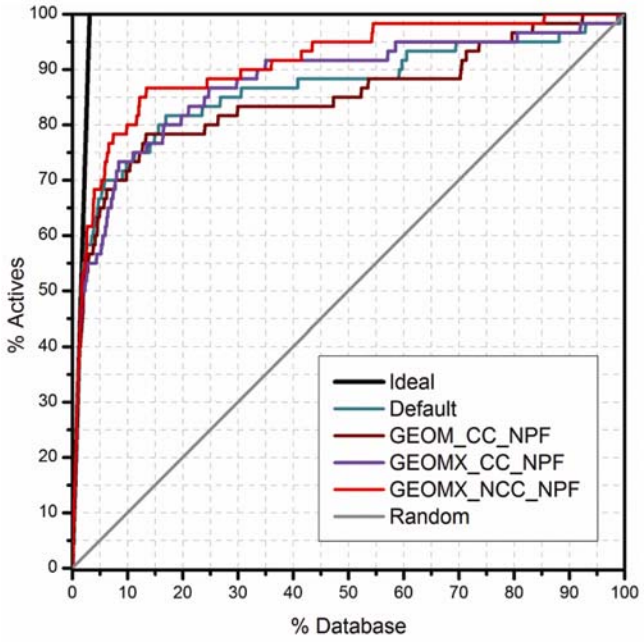

Figure 6. Enrichment curves showing the recovery of HIV-1 protease active inhibitors using 'Default' docking mode. Four sets of docking parameters were used corresponding to the default scoring function (dark green) and three customized scoring functions. The AUC (area under the curve) values are as follows: Default (0.85), GEOM_CC_NPF (0.84), GEOMX_CC_NPF (0.86) and GEOMX_NCC_NPF (0.90).

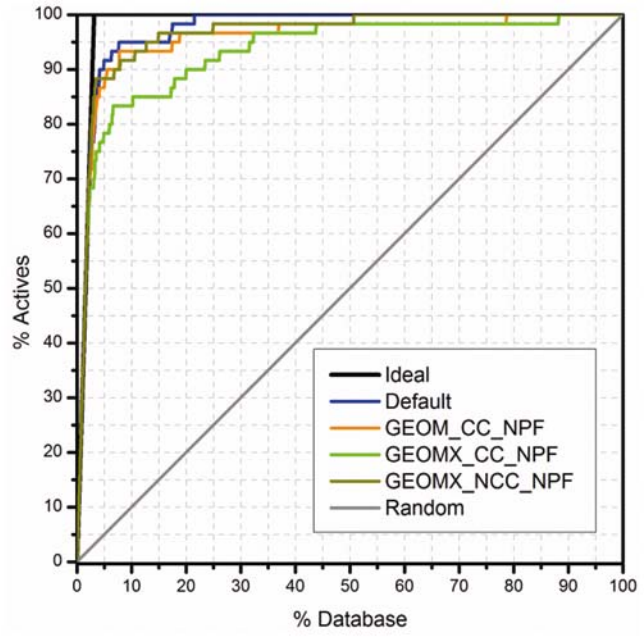

Figure 7. Enrichment curves showing the recovery of HIV-1 protease active inhibitors using 'GEOM' docking mode. Four sets of docking parameters were used corresponding to the default scoring function (blue) and three customized scoring functions. The AUC values are as follows: Default (0.96), GEOM_CC_NPF (0.94), GEOMX_CC_NPF (0.92) and GEOMX_NCC_NPF (0.95).

At the suggestion of one of the reviewers, we have studied the possibility of obtaining better correlations with experimental data by the individual contributions to the total score. We would like to emphasize that in the case of the Surflex-dock scoring function, such contributions

Table 5. Correlation factors between experimental pK_i and docking scores obtained from customized scoring functions using top 5 docked poses for each of the nine ligands in TRGSET. The columns labelled CC and PF correspond to the usage of 'core constraints' and 'protein flexibility' in the docking protocols. Correlations corresponding to average scores, maximum scores, minimum scores, top-ranked scores, and mean of minimum and maximum scores are shown in columns 4–7 respectively. The last column depicts the gain in correlation factor due to customization based on the highest correlation for a given docking protocol

Docking mode	CC	PF	Average	Maximum	Minimum	MMB2	Top rank	Highest	Default parameters	Gain
DEFAULT	No	No	0.29	0.28	0.24	0.30	0.41	0.41	0.17	0.24
	No	Yes	–0.64	–0.37	–0.49	–0.54	–0.29	–0.29	–0.47	0.17
	Yes	No	0.54	0.62	0.08	0.38	0.57	0.62	0.62	0.00
	Yes	Yes	0.20	–0.05	0.39	0.28	0.16	0.39	–0.18	0.57
GEOM	No	No	0.32	0.19	0.53	0.37	0.33	0.53	0.39	0.14
	No	Yes	0.30	0.17	–0.28	–0.10	0.38	0.38	0.37	0.01
	Yes	No	0.61	0.50	0.59	0.58	0.46	0.61	0.37	0.24
	Yes	Yes	0.68	0.17	0.44	0.53	0.49	0.68	0.69	–0.01
GEOMX	No	No	0.60	0.39	0.65	0.62	0.20	0.65	0.38	0.27
	No	Yes	0.57	0.49	0.31	0.63	0.19	0.63	0.74	–0.11
	Yes	No	0.49	0.36	0.39	0.50	0.18	0.50	0.13	0.37
	Yes	Yes	0.66	0.31	0.77	0.64	0.26	0.77	0.74	0.03
SCREEN	No	No	0.17	0.36	–0.03	0.17	0.40	0.40	0.04	0.36
	No	Yes	0.35	0.61	–0.05	0.34	0.06	0.61	0.38	0.23
	Yes	No	0.56	0.45	0.52	0.52	0.40	0.56	0.42	0.14
	Yes	Yes	0.62	0.65	0.13	0.44	0.20	0.65	–0.24	0.89

are constituted by electrostatic, van der Waals (steric/hydrophobic) and entropic terms and that terms such as π-stacking, hydrogen bonding, hydrophobic enclosure, etc. are not evaluated explicitly (as they are considered implicitly embedded in the simpler electrostatic and van der Waals terms). Our analyses indicate that the correlations between the experimental data on the one hand and the three individual contributions on the other, are generally no better than the correlations with the total scores. Of the three, the electrostatic terms have the best correlations in general. However, their values are less than or equal to the correlation factors obtained with the total scores. The contributions to total binding by more specific interactions as π-stacking, hydrogen bonding, hydrophobic enclosure are being currently evaluated using alternative docking software methods and are beyond the scope of this article. They will be discussed in detail in a future publication. The preliminary analyses also demonstrate no special advantage for the individual contributions (unpublished data).

In light of the poor correlation between the experimental observations and computed docking scores (as discussed above), we customized the scoring function of Surflex-dock by tuning it to the reported pK_i values of the TRGSET compounds. Correlation factors obtained using customized scoring functions are shown in Table 5. Correlation factors obtained by five different metrics (as outlined earlier in the article and tabulated in columns marked 'Average', 'Max', 'Min', 'MMB2' and 'Top Rank') are shown in Table 5. In addition, the column labelled 'Highest' shows the maximum correlation obtained by any metric and the column 'Gain' shows the increase in correlation factor due to customization of scoring function (by considering the highest value obtained). In the case of GEOM and GEOMX docking modes, customization does lead to larger improvements in correlation factors when post-docking protein flexibility is not included. However, the scoring function customization does not marginally appreciate when PDPF is included in the docking protocol. In fact, in the case of GEOMX docking mode, the default scoring function yields better correlation than any of the metrics computed using customized scoring function when PDPF is included. Scoring function customization has maximal benefit on the correlations obtained for screening and default modes of docking with the inclusion of PDPF and core constraints (gain of 0.89 and 0.57 respectively). On the other hand, it has only modest impact on correlations obtained with scores from docking studies without incorporating PDPF. In addition, we have also examined the impact of increasing the number of refinement cycles (option '-repeat') in the scoring function optimization process. Changing this value from 5 to 10 and 25 did not seem to alter the correlation factors significantly (less than 0.05). In response to a suggestion made by one of the reviewers, we would like to add that the approach of tuning the scoring function (that is unique to Surflex-dock scoring function) for improving binding predictions can be applicable widely wherever appropriate amount of experimental data are available, but cannot be correlated directly to the computed docking scores. Typically, pIC_{50} values are harder to correlate with docking scores compared to pK_i values and in such cases, a customized and tuned scoring function would be especially useful in designing compounds belonging to specific chemotypes as enzyme inhibitors.

Based on the above reported analyses, we have chosen three of the customized scoring functions corresponding to (a) GEOM docking with core constraints and no PDPF,

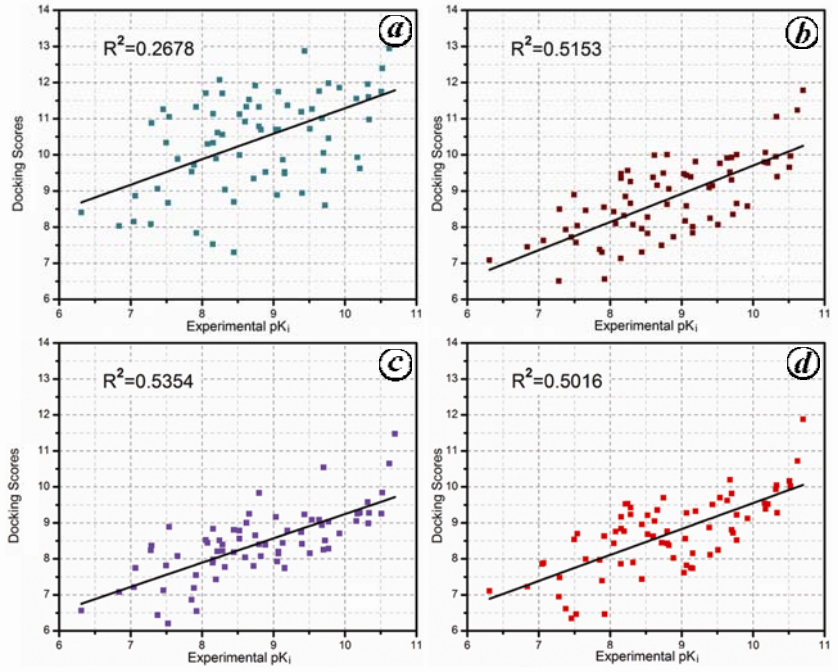

Figure 8. Correlation plots between experimental pK_i values of HIV-1 protease inhibition and 'Default mode' Surflex docking scores obtained with (***a***) Default, (***b***) GEOM_CC_NPF, (***c***) GEOMX_CC_NPF and (***d***) GEOMX_NCC_NPF parameters. The *R*-squared values of the trend lines of these distributions are also shown.

(b) GEOMX docking with core constraints and no PDPF and (c) GEOMX docking with no core constraints and no PDPF. We have used these scoring functions to see if they will have any impact on the enrichments of actives discussed earlier. Figures 6 and 7 show the enrichment plots for the recovery of the actives obtained by the DEFAULT and GEOM modes of docking respectively. In each figure, the enrichment plots were obtained with the default scoring function and the aforementioned three customized scoring functions. The raw data corresponding to these plots are given under '**Supplementary Material**', which shows the percentage of actives recovered in each percentage of the total database studied.

In these screening studies, as indicated earlier, no core constraints and PDPF were employed. It is seen that the usage of custom scoring functions derived from the poses of GEOMX docking with and without core constraints has positive impacts on the recovery of actives when the virtual screening is carried out using Default docking mode (Figure 6). Interestingly, in this case, the custom scoring function obtained from poses of GEOM docking have a somewhat negative impact on the enrichment compared to the default scoring function. Interestingly, all the four scoring functions show similar early enrichments as seen by the steep rise in the plots from 0% to 2% of the databases screened. Interestingly, in the case of virtual docking by GEOM docking method, the best enrichment is obtained by the default scoring function, although the enrichments obtained by two of the three custom scoring functions are similar. The scoring function obtained from poses of GEOMX docking with core constraints leads to appreciable deterioration of enrichment in this mode of virtual screening. Thus, these studies indicate the potential benefit of the customized scoring function on screening of actives when the faster default mode of docking is employed. This may not be entirely surprising since the GEOM mode of screening even with the default scoring function discriminates actives from the decoys reliably and the customization does not seem to contribute anything substantial to that behaviour.

In addition to the enrichment studies, we have analysed the effects of employing the customized scoring functions on the correlation between computed docking scores and experimental pK_i values for a series of HIV-1 protease inhibitors whose activity values span more than four orders of magnitude (TESTSET2). The pK_i values of the 71 compounds in TESTSET2 range from 6.3 to 10.7 (Table 2). It may be noted that the stereochemistry at the four chiral carbon atoms in all these molecules is maintained in the configuration present in molecule **1** of TRGSET (Figure 1) in light of its highest activity. Their docking scores, also listed in Table 2, were obtained using the 'Default' mode of Surflex docking without incorporating any post-docking protein flexibility and core constraints. The docking experiment was carried out in the spirit of high throughput virtual screening where the imposition of such additional constraints would not necessarily be practical.

The correlations between the experimental pK_i and docking scores are illustrated in Figure 8. As observed in these plots, the *R*-squared values of the correlations are

improved from 0.26 (in the plot corresponding to default scoring function) to values greater than 0.5 upon the utilization of the customized scoring functions. This observation is significant in light of the fact that the scoring functions were derived from a much simpler training set of molecules which do not have the range of substituents on the cyclic urea core as seen in TESTSET2 molecules.

Conclusion

We have presented Surflex docking studies in the active site of HIV-1 protease as a function of various docking parameters such as incorporation of protein flexibility, core constraints and docking accuracy levels. We have carried out customization of Surflex-dock scoring function using a training set of cyclic urea inhibitors whose binding affinities span a little over three orders of magnitude. We have demonstrated that such customization does lead to improvement in the correlation of docking scores with the experimental data. We find that the customized scoring functions are helpful in improving the correlation between docking scores and experimental binding affinities for an external test set of HIV-1 protease inhibitors whose activities span more than four orders of magnitude. We have also demonstrated that in high-throughput virtual screening, the customized scoring functions have enhancing effects on the ability of the docking scores to recover active ligands seeded in a database of decoy molecules when lower accuracy docking methods are employed. The present study clearly illustrates the potential utility of scoring function customization in docking-based approaches that are commonly used in drug discovery workflows.

Supporting information

Raw data corresponding to the enrichment plots in Figures 6 and 7 are listed in Table 6 under Supporting Material (available online), which shows the percentage of actives recovered as a function of the percentage of databases ranked on the basis of total docking score. The three-dimensional coordinates of the ligands listed in Tables 1 and 5 are provided in structure-data (SD) formatted files. This material is available free of charge on the *Current Science* website.

1. Glick, M. and Jacoby, E., The role of computational methods in the identification of bioactive compounds. *Curr. Opin. Chem. Biol*., 2011, **15**, 540–546.
2. Funatsu, K., Miyao, T. and Arakawa, M., Systematic generation of chemical structures for rational drug design based on QSAR models. *Curr. Comput. Aided Drug Des*., 2011, **7**, 1–9.
3. Ebalunode, J. O., Zheng, W. and Tropsha, A., Application of QSAR and shape pharmacophore modeling approaches for targeted chemical library design. *Methods Mol. Biol*., 2011, **685**, 111–133.
4. Koppen, H., Virtual screening – what does it give us? *Curr. Opin. Drug Discov. Devel*., 2009, **12**, 397–407.
5. Cerqueira, N. M., Sousa, S. F., Fernandes, P. A. and Ramos, M. J., Virtual screening of compound libraries. *Methods Mol. Biol*., 2009, **572**, 57–70.
6. McInnes, C., Virtual screening strategies in drug discovery. *Curr. Opin. Chem. Biol*., 2007, **11**, 494–502.
7. Schwardt, O., Kolb, H. and Ernst, B., Drug discovery today. *Curr. Top. Med. Chem*., 2003, **3**, 1–9.
8. Ma, X. H., Comparative analysis of machine learning methods in ligand-based virtual screening of large compound libraries. *Comb. Chem. High Throughput Screen*, 2009, **12**, 344–357.
9. Klabunde, T. and Jager, R., Chemogenomics approaches to G-protein coupled receptor lead finding. *Ernst Schering Res. Found. Workshop*, 2006, 31–46.
10. Klebe, G., Recent developments in structure-based drug design. *J. Mol. Med.* (*Berl.*), 2000, **78**, 269–281.
11. Brooks, W. H., Guida, W. C. and Daniel, K. G., The significance of chirality in drug design and development. *Curr. Top. Med. Chem*., 2011, **11**, 760–770.
12. Schneider, G., Trends in virtual combinatorial library design. *Curr. Med. Chem*., 2002, **9**, 2095–2101.
13. Tropsha, A. and Golbraikh, A., Predictive QSAR modeling workflow, model applicability domains, and virtual screening. *Curr. Pharm. Des*., 2007, **13**, 3494–3504.
14. Cramer, R. D., Cruz, P., Stahl, G., Curtiss, W. C., Campbell, B., Masek, B. B. and Soltanshahi, F., Virtual screening for R-groups, including predicted pIC_{50} contributions, within large structural databases, using Topomer CoMFA. *J. Chem. Inf. Model.*, 2008, **48**, 2180–2195.
15. Giganti, D., Guillemain, H., Spadoni, J. L., Nilges, M., Zagury, J. F. and Montes, M., Comparative evaluation of 3D virtual ligand screening methods: impact of the molecular alignment on enrichment. *J. Chem. Inf. Model.*, 2010, **50**, 992–1004.
16. Lemmen, C. and Lengauer, T., Computational methods for the structural alignment of molecules. *J. Comput. Aided Mol. Des*., 2000, **14**, 215–232.
17. Zhong, S., Zhang, Y. and Xiu, Z., Rescoring ligand docking poses. *Curr. Opin. Drug Discov. Devel*., 2010, **13**, 326–334.
18. Waszkowycz, B., Towards improving compound selection in structure-based virtual screening. *Drug Discov. Today*, 2008, **13**, 219–226.
19. Kontoyianni, M., Madhav, P., Suchanek, E. and Seibel, W., Theoretical and practical considerations in virtual screening: a beaten field? *Curr. Med. Chem*., 2008, **15**, 107–116.
20. Kroemer, R. T., Structure-based drug design: docking and scoring. *Curr. Protein Pept. Sci*., 2007, **8**, 312–328.
21. Kitchen, D. B., Decornez, H., Furr, J. R. and Bajorath, J., Docking and scoring in virtual screening for drug discovery: methods and applications. *Nature Rev. Drug Discov*., 2004, **3**, 935–949.
22. Jansen, J. M. and Martin, E. J., Target-biased scoring approaches and expert systems in structure-based virtual screening. *Curr. Opin. Chem. Biol*., 2004, **8**, 359–364.
23. Fradera, X. and Mestres, J., Guided docking approaches to structure-based design and screening. *Curr. Top. Med. Chem*., 2004, **4**, 687–700.
24. Jain, A. N., Surflex: fully automatic flexible molecular docking using a molecular similarity-based search engine. *J. Med. Chem.*, 2003, **46**, 499–511.
25. Miteva, M. A., Lee, W. H., Montes, M. O. and Villoutreix, B. O., Fast structure-based virtual ligand screening combining FRED, DOCK, and Surflex. *J. Med. Chem*., 2005, **48**, 6012–6022.
26. Plewczynski, D., Lazniewski, M., von Grotthuss, M., Rychlewski, L. and Ginalski, K., VoteDock: consensus docking method for prediction of protein–ligand interactions. *J. Comput. Chem*., 2011, **32**, 568–581.

27. Plewczynski, D., Lazniewski, M., Augustyniak, R. and Ginalski, K., Can we trust docking results? Evaluation of seven commonly used programs on PDBbind database. *J. Comput. Chem*., 2011, **32**, 742–755.
28. Jain, A. N., Effects of protein conformation in docking: improved pose prediction through protein pocket adaptation. *J. Comput. Aided Mol. Des*., 2009, **23**, 355–374.
29. Pham, T. A. and Jain, A. N., Customizing scoring functions for docking. *J. Comput. Aided Mol. Des*., 2008, **22**, 269–286.
30. Thomsen, R. and Christensen, M. H., MolDock: a new technique for high-accuracy molecular docking. *J. Med. Chem*., 2006, **49**, 3315–3321.
31. Kellenberger, E., Rodrigo, J., Muller, P. and Rognan, D., Comparative evaluation of eight docking tools for docking and virtual screening accuracy. *Proteins*, 2004, **57**, 225–242.
32. Jain, A. N., Surflex-dock 2.1: robust performance from ligand energetic modeling, ring flexibility, and knowledge-based search. *J. Comput. Aided Mol. Des*., 2007, **21**, 281–306.
33. Pearlstein, R. A. *et al.*, New hypotheses about the structure–function of proprotein convertase subtilisin/kexin type 9: analysis of the epidermal growth factor-like repeat A docking site using WaterMap. *Proteins*, 2010, **78**, 2571–2586.
34. Huggins, D. J., Sherman, W. and Tidor, B., Rational approaches to improving selectivity in drug design. *J. Med. Chem*., 2012, **55**, 1424–1444.
35. Beuming, T., Che, Y., Abel, R., Byungchan, K., Shanmugasundaram, V. and Sherman, W., Thermodynamic analysis of water molecules at the surface of proteins and applications to binding site prediction and characterization. *Proteins*, 2012, **80**, 871–883.
36. Jain, A. N., Virtual screening in lead discovery and optimization. *Curr. Opin. Drug Discov. Devel*., 2004, **7**, 396–403.
37. SYBYL-X 1.3, Tripos International, St Louis, Missouri, USA.
38. Kaltenbach III, R. F., Nugiel, D. A., Lam, P. Y., Klabe, R. M. and Seitz, S. P., Stereoisomers of cyclic urea HIV-1 protease inhibitors: synthesis and binding affinities. *J. Med. Chem*., 1998, **41**, 5113–5117.
39. Jadhav, P. K., Ala, P., Woerner, F. J., Chang, C. H., Garber, S. S., Anton, E. D. and Bacheler, L. T., Cyclic urea amides: HIV-1 protease inhibitors with low nanomolar potency against both wild type and protease inhibitor resistant mutants of HIV. *J. Med. Chem*., 1997, **40**, 181–191.
40. Berman, H. M. *et al.*, The Protein Data Bank. *Nucl. Acids Res*., 2000, **28**, 235–242.
41. Bone, R., Vacca, J. P., Anderson, P. S. and Holloway, M. K., X-ray crystal structure of the HIV protease complex with L-700,417, an inhibitor with pseudo C2 symmetry. *J. Am. Chem. Soc*., 1991, **113**, 9382–9384.
42. Clark, M., Cramer III, R. D. and Van Opdenbosch, N., Validation of the general purpose tripos 5.2 force field. *J. Comp. Chem*., 1989, **10**, 21.
43. Pearlman, R. S., 'Concord' distributed by Tripos International, St Louis, Missouri, USA.
44. Rodgers, J. F. and Johnson, B. L., Potent cyclic urea HIV protease inhibitors with 3-aminoindazole P2/P2′ groups. *Bioorg. Med. Chem. Lett*., 1998, **8**, 715–720.
45. Wilkerson, W. W. *et al.*, HIV protease inhibitory bis-benzamide cyclic ureas: a quantitative structure–activity relationship analysis. *J. Med. Chem*., 1996, **39**, 4299–4312.
46. De Lucca, G. V. *et al.*, Design, synthesis, and evaluation of tetrahydropyrimidinones as an example of a general approach to nonpeptide HIV protease inhibitors. *J. Med. Chem*., 1997, **40**, 1707–1709.
47. Wilkerson, W. W., Dax, S. and Cheatham, W. W., Nonsymmetrically substituted cyclic urea HIV protease inhibitors. *J. Med. Chem*., 1997, **40**, 4079–4088.
48. De Lucca, G. V. *et al.*, Nonsymmetric P2/P2′ cyclic urea HIV protease inhibitors. Structure–activity relationship, bioavailability, and resistance profile of monoindazole-substituted P2 analogues. *J. Med. Chem*., 1998, **41**, 2411–2423.
49. Han, Q., Chang, C.-H., Li, R., Ru, Y., Jadhav, P. K. and Lam, P. Y., Cyclic HIV protease inhibitors: design and synthesis of orally bioavailable, pyrazole P2/P2′ cyclic ureas with improved potency. *J. Med. Chem*., 1998, **41**, 2019–2028.
50. Patel, M., Bacheler, L. T., Rayner, M. M., Cordova, B. C., Klabe, R. M., Erickson-Viitanen, S. and Seitz, S. P., The synthesis and evaluation of cyclic ureas as HIV protease inhibitors: modifications of the P1/P1′ residues. *Bioorg. Med. Chem. Lett*., 1998, **8**, 823–828.
51. Patel, M. *et al.*, The synthesis of symmetrical and unsymmetrical P1/P1′ cyclic ureas as HIV protease inhibitors. *Bioorg. Med. Chem. Lett*., 1998, **8**, 1077–1082.
52. Rodgers, J. D. *et al.*, Potent cyclic urea HIV protease inhibitors with 3-aminoindazole P2/P2′ groups. *Bioorg. Med. Chem. Lett*., 1998, **8**, 715–720.
53. De Lucca, G. V., Liang, J. and De Lucca, I., Stereospecific synthesis, structure–activity relationship, and oral bioavailability of tetrahydropyrimidin-2-one HIV protease inhibitors. *J. Med. Chem*., 1999, **42**, 135–152.
54. Debnath, A. K., Three-dimensional quantitative structure–activity relationship study on cyclic urea derivatives as HIV-1 protease inhibitors: application of comparative molecular field analysis. *J. Med. Chem*., 1999, **42**, 249–259.
55. Kaltenbach III, R. F., Klabe, R. M., Cordova, B. C. and Seitz, S. P., Increased antiviral activity of cyclic urea HIV protease inhibitors by modifying the P1/P1′ substituents. *Bioorg. Med. Chem. Lett*., 1999, **9**, 2259–2262.
56. Patel, M. *et al.*, Unsymmetrical cyclic ureas as HIV-1 protease inhibitors: novel biaryl indazoles as P2/P2′ substituents. *Bioorg. Med. Chem. Lett*., 1999, **9**, 3217–3120.
57. Kaltenbach III, R. F. *et al*., Synthesis, antiviral activity and pharmacokinetics of P1/P1′ substituted 3-aminoindazole cyclic urea HIV protease inhibitors. *Bioorg. Med. Chem. Lett*., 2003, **13**, 605–608.
58. Rodgers, J. D. *et al.*, Potent cyclic urea HIV protease inhibitors with benzofused heterocycles as P2/P2′ groups. *Bioorg. Med. Chem. Lett*., 1996, **6**, 2919–2924.
59. Jain, A. N., Bias, reporting, and sharing: computational evaluations of docking methods. *J. Comput. Aided Mol. Des*., 2008, **22**, 201–212.
60. Nugiel, D. A. *et al.*, Preparation and structure–activity relationship of novel P1/P1′-substituted cyclic urea-based human immunodeficiency virus type-1 protease inhibitors. *J. Med. Chem*., 1996, **39**, 2156–2169.
61. Smallheer, J. M. *et al.*, Functionalized aliphatic P2/P2′ analogs of HIV-1 protease inhibitor DMP323. *Bioorg. Med. Chem. Lett*., 1997, **7**, 1365–1370.
62. Lam, P. Y. *et al.*, Cyclic HIV protease inhibitors: synthesis, conformational analysis, P2/P2′ structure–activity relationship, and molecular recognition of cyclic ureas. *J. Med. Chem*., 1996, **39**, 3514–3525.
63. Jadhav, P. K. *et al.*, Nonpeptide cyclic cyanoguanidines as HIV-1 protease inhibitors: synthesis, structure–activity relationships, and X-ray crystal structure studies. *J. Med. Chem*., 1998, **41**, 1446–1455.
64. Nugiel, D. A. *et al.*, Improved P1/P1′ substituents for cyclic urea based HIV-1 protease inhibitors: synthesis, structure–activity relationship, and X-ray crystal structure analysis. *J. Med. Chem*., 1997, **40**, 1465–1474.

ACKNOWLEDGEMENTS. We thank Prof. Ajay N. Jain (UCSF) for valuable suggestions on various command line options in the customization of Surflex-dock scoring function. We also thank the reviewers for their useful suggestions.

Received 6 July 2012; revised accepted 30 November 2012